Hindawi
Advances in Polymer Technology
Volume 2023, Article ID 7276854, 9 pages
https://doi.org/10.1155/2023/7276854

Research Article

Thermo-Responsive Shape Memory Thermoplastic Elastomer Based on Natural Rubber and Ethylene Octene Copolymer Blends

Ekwipoo Kalkornsurapranee[1], **Adisak Keereerak**[1,2], **Nussana Lehman**[1], **Akarapong Tuljittraporn**[1], **Jobish Johns**[3] and **Nattapon Uthaipan**[2]

[1]*Division of Physical Science, Faculty of Science, Prince of Songkla University, Songkhla 90110, Thailand*
[2]*Rubber Technology and Engineering Program, International College, Prince of Songkla University, Songkhla 90110, Thailand*
[3]*Department of Physics, Rajarajeswari College of Engineering, Bengaluru 560074, India*

Correspondence should be addressed to Nattapon Uthaipan; nattapon.u@psu.ac.th

Received 2 June 2022; Revised 4 September 2023; Accepted 5 October 2023; Published 30 October 2023

Academic Editor: Kavimani V.

The shape memory (SM) polymers with superior SM properties were successfully fabricated based on melt blending of natural rubber (NR) and ethylene octene copolymer (EOC) at various crystallinity of EOC phase. The differential scanning calorimetry analysis, mechanical properties, temperature scanning stress relaxation, and shape memory properties were studied. Results revealed that the mechanical and thermal properties of the prepared NR/EOC blends improved as a function of amount of ethylene fraction in the EOC phase. The ethylene segment of EOC in the NR/EOC blend is triggered as a stimulus-sensitive domain. The shape memory properties in terms of shape fixity and shape recovery efficiencies of the blends tended to increase with the increasing of crystalline segments in the blends. The shape memory properties of the prepared blends substantially exceed the best performance (close to 100%) by blending the NR/EOC at 50/50 parts by weight, having 62%–80% of ethylene content in the EOC phase, which corresponds to approximately 3°–16° of crystallinity of EOC phase in the blends.

1. Introduction

Shape memory polymers (SMPs) are currently being highlighted both in academic and industrial fields with tremendous development due to its various functionalities [1, 2]. SMPs are smart or intelligent materials that can recover a temporary shape to its original (memorized) shape when subjected to an external stimulus such as chemical, temperature, electricity, and magnetic field without applying an external force [3–5]. Among those developed SMPs, thermo-responsive SMP is a typical kind of SMPs, which has been widely studied and used in industry practices [6, 7].

In general, at the molecular level, thermo-responsive SMPs are the possession of molecular switching segments and net points. Net points are responsible for determining the permanent shape, while the switching segments are responsible for shape shifting process [8, 9]. The behavior of the SMP can be controlled by a transition temperature (T_{trans}), which is related to either the melting temperature (T_m) for a semicrystalline polymer or the glass transition temperature (T_g) for an amorphous polymer [1, 10, 11]. The SMP is deformed in the amorphous state to an elongation by application of external stress, generally, above a transition temperature, and fixed in the desired temporary shape by cooling the material to a crystallization temperature (T_c) of switching domains; these domains solidify acting as a physical cross-linking [12].

During the last decade, the SMPs based on high-density polyethylene (HDPE) and polyethylene terephthalate, cross-linked linear-low density polyethylene/polypropylene, and HDPE-short chain with branched polyethylene, i.e., ethylene-1-octene copolymers (EOC) have been developed [13–16]. Natural rubber (NR) is a biopolymer having unique chemical and physical properties, i.e., high elasticity, good mechanical properties, especially excellent strain-induced crystallization (SIC) behaviors. For these reasons, the NR is considered a potential raw material for SMPs. [17, 18]. An amorphous structure in NR is able to turn into crystalline form upon

Table 1: Specifications of EOCs [19, 20].

Specifications	EOC grades			
	8842	8100	8003	8480
Ethylene content (wt%)	55	62	70	80
Octene content (wt%)	45	38	30	20
MFI (g/10 min)	1	1	1	1
Crystallinity (%)	13	18	25	33
Density (g/cm^3)	0.857	0.870	0.885	0.902
Hardness (shore A)	54	73	84	89
Glass transition temperature (°C)	−58	−52	−46	−31
Melting temperature (°C)	38	60	77	99
Solubility parameter (J/cm^3)$^{1/2}$	17.2	17.3	17.5	17.6

strain. This phenomenon is known as SIC that occurs at room temperature and disappears when the applied force is released [16]. Cross-linked NR can also be used as SMPs with the capacity to store large strains. It has been reported that NR-based SMPs can store a strain of up to 1,000% [17]. Therefore, many researchers have been interested in developing SMPs based on NR (NR-based SMPs). Some of the NR-based SMPs were used in forensic applications (block-copolymer-based polyolefin) and splint fabrication based on epoxidized rubber (NR/ENR combined with poly(caprolactone)) [4, 5].

In the present work, the blends of NR/EOCs were prepared through the melt blending method. NR was used as the switching phase, while EOCs were employed as a thermoplastic counterpart (net point) with various degrees of crystallinity (13%–33%). Mechanical and thermal properties, stress relaxation behavior, Mooney–Rivlin model, shape memory (the shape fixity efficiency and the shape recovery efficiency), and the recyclability of the investigated NR/EOC blends were discussed in detail.

2. Materials and Methods

2.1. Materials. NR (standard Thai rubber, grade 5L; STR 5L) was purchased from Chalong Latex Industry Co., Ltd., Thailand. Ethylene octene copolymers (EOCs, trade name Engage, with the ranging of octene content from 5.9 to 16.9 mol%) were supplied by DuPont Dow Elastomer Co., Ltd., United States. Specifications of the EOCs are compiled in Table 1. Calcium carbonate ($CaCO_3$) used as a filler was manufactured by C.P. Chemical Industry Co., Ltd., Thailand. Paraffinic oil was supplied by the Petroleum Authority of Thailand (PTT) Oil and Retail Business Public Co., Ltd., Thailand. Titanium dioxide (TiO_2) was manufactured by DuPont Company, USA.

2.2. Preparation of NR/EOC Blends. NR/EOC blends were prepared via melt compounding method at a constant NR/EOC ratio of 50/50 wt% with various EOC grades, i.e., 8842, 8100, 8003, and 8480. The NR compound was firstly prepared using a two roll mill (ML-D6L12, CT, Thailand) in which the chemical ingredients were computed based on 100 parts of rubber, as shown in Table 2. After completion of NR compounding, the NR compound was melt-mixed with EOC in an internal mixer (Rheo drive 7 OS, Haake, Germany). In the blending step, the EOC was initially added into the mixing chamber at a mixing temperature of 100°C, rotor speed of 60 rpm, and then melted for 2 min. After that, the NR compound was incorporated into the chamber and continued mixing for another 4 min. After that, the NR compound was incorporated into chamber 96 and continued mixing for another 4 min. After finishing blending, the prepared NR/EOC blend 97 was immediately removed from the mixing chamber and sheeted out on a two roll mill to 98 to prepare a pre-form before fabrication. A sheet specimen with a thickness of 2 mm was prepared 99 using compression molding (SLLP-50, SiamLab, Thailand) at a temperature of 100°C. The 100 preheating, pressing, and cooling times were set at 7, 7, and 5 min, respectively.

Table 2: Formulation of NR compound.

Ingredients	Quantities (phr)
STR 5L	100
$CaCO_3$	100
Paraffinic oil	10
TiO_2	10

3. Tests and Characterization

3.1. Differential Scanning Calorimetry (DSC) Studies. DSC studies of the NR/EOC blends were done in a DSC3+ (Mettler Toledo AG, Switzerland) with applying a program of heating and cooling under N_2 atmosphere. To remove the thermal history, the sample (5–10 mg) was heated from 20 to 250°C at a heating rate of 10°C/min. Then, the sample was cooled down to 20°C at a cooling rate of 10°C/min to investigate the crystallization temperature (T_c) obtained from the maximum peak area of the cooling scan. Finally, the sample was heated again from 20 to 250°C to obtain the melting curve, including melting temperature (T_m) and heat of fusion of the crystalline segment. The degree of crystallinity (X_c) was obtained from the second heating scan and was determined according to Equation (1) [21].

$$X_C = \frac{\Delta H_f}{\Delta H_{f0} \times W} \times 100. \quad (1)$$

In the above equation, ΔH_f represents the fusion (melting) enthalpy obtained from the DSC curve, ΔH_{f0} represents the theoretical fusion enthalpy of 100% crystalline polyethylene (293 J/g) [21], and W represents the weight fraction of EOC in the polymer blend.

3.2. Mechanical Properties. Tensile properties of the NR/EOC blends, including 100% modulus, tensile strength, and elongation at break, were performed according to ASTM D412 on a universal testing machine (EX800Plus, LLOYD, United States) using a dumbbell shape specimen (type II, ISO37) at a crosshead speed of 500 mm/min. A hardness test was carried out according to ASTM D2240 using Shore A durometer (BS61 II, Bareiss, Germany).

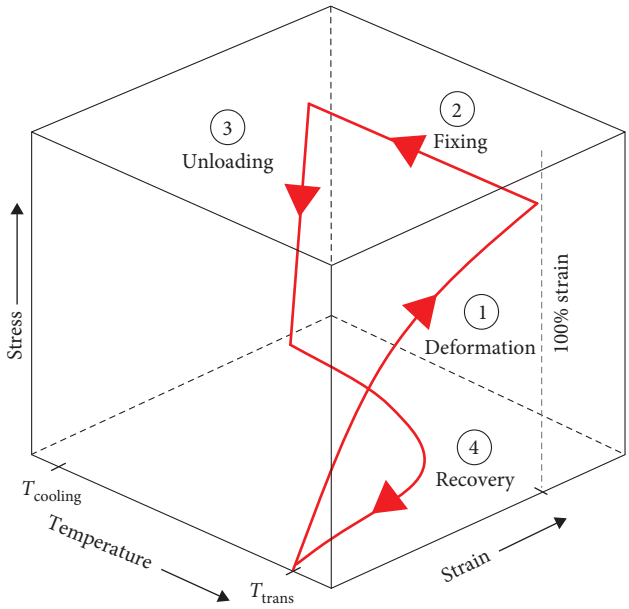

FIGURE 1: Procedure to measure the shape memory properties of NR/EOC blends.

3.3. Dynamic Mechanical Analysis. Thermal analysis of the NR/EOC blends was performed with a dynamic mechanical analyzer (DMA1, Mettler Toledo, Switzerland). The test was carried out in tension mode at a heating rate of 5°C/min and a constant strain of 0.1%. The samples were scanned across the temperature range from −100 to 100°C, and the frequency was set at 5 Hz.

3.4. The Morphological Analysis. The fracture surface of the NR/EOC blends was conducted with a scanning electron microscope (SEM, FEI Quanta 400, the Netherlands). The samples were fractured in liquid nitrogen and vapor stained with osmium tetroxide (OsO_4) in order to increase phase contrast. The samples were tested under back-scattering mode (SEM-BSE).

3.5. SM Properties. The test method, according to Tekay [21], was adopted to study the shape memory properties of SMPs. The rectangular shape specimen with a dimension of $10 \times 30 \times 20\ mm^3$ was die-cut from the molded sheet. An adjustable clamp was used to measure the shape memory properties of the TPNR sample applied by uniaxial tension. The test procedure was performed in four steps as illustrated in Figure 1; (1) Deformation: the sample with an initial gauge length of 10 mm (l_i) was softened in water bath at various testing temperatures (i.e., 30, 40, 50, 60, 70, 80, and 90°C) for 2 min and then stretched to 100% strain; (2) Shape fixity: the deformed sample on an adjustable clamp was immediately quenched in cold water at 10°C for 5 min to obtain a temporary shape (finished quench) (l_m); (3) Force removing: the sample was removed from the clamp (removed bolt-on clamp) and allowed to recover for 10 min at ambient temperature to measure the fixed length (l_f); and (4) Shape recovery: the fixed-length sample was again immersed in water bath at the testing temperature for 30 min. After complete recovery, the recovery length (l_r) of the sample was measured. The shape fixity (R_f) and shape recovery (R_r) efficiency of NR/EOC blends were calculated by means of Equations (2) and (3):

$$R_f = \frac{l_f}{l_m} \times 100, \tag{2}$$

$$R_r = \frac{l_f - l_r}{l_f - l_i} \times 100, \tag{3}$$

where l_m and l_f represent the maximum length at high temperatures and the length under stress-free conditions at low temperatures, respectively. l_r represents the length of the deformed sample after recovery for 30 min, and l_i represents the initial gauge length of the sample before the deformation of sample.

3.6. Temperature Scanning Stress Relaxation. Temperature scanning stress relaxation experiments, both isothermal and nonisothermal relaxations of NR/EOC blends, were performed by a temperature scanning stress relaxation (TSSR) instrument (Brabender® TSSR meter, Brabender Gmbh, Germany) equipped with an electrical heating chamber and adjusted deformation device. The isothermal relaxation measured at 23°C with an initial strain of 50% for 2 hr is executed to eliminate of the negative contribution of stress relaxation of the sample. After that, a nonisothermal test was performed by raising the temperature with a constant heating rate of 2°C/min. The sample was continually stretched until the complete relaxation process or rupture of the sample took place. From TSSR measurement, thermoelastic inversion point (T_{10}), compression set resistance (T_{50}), and material stability (T_{90}) have been measured using the normalized force–temperature curve at which the force (F) has decreased from its initial value (F_0) by 10%, 50%, and 90%, respectively. Rubber index (RI) indicates the elastomeric behavior of the material is calculated by the area below the normalized force–temperature curve.

4. Results and Discussion

4.1. DSC Analysis. The thermal properties, including crystallization temperature, melting temperature, and degree of crystallinity of EOC phase in NR/EOC blends, were determined by DSC measurement. The DSC thermograms (melting and cooling peaks) are given in Figure 2.

It is clearly seen that the melting and crystallization of EOC phase in the NR/EOC blend are much affected by the type of EOC in the prepared blends. The polyethylene backbone is a crystalline segment, whereas the presence of the octene comonomer in EOC causes a lower level of crystallinity and a higher flexibility in the copolymer [20]. In a comparison of the EOC types, the melting and cooling peaks of EOC phase in NR/EOC blends shifted forward to high temperature as the amount of ethylene hard block increased. The crystalline fraction of ethylene comonomer in the prepared NR/EOC blends was melted approximately in the range of

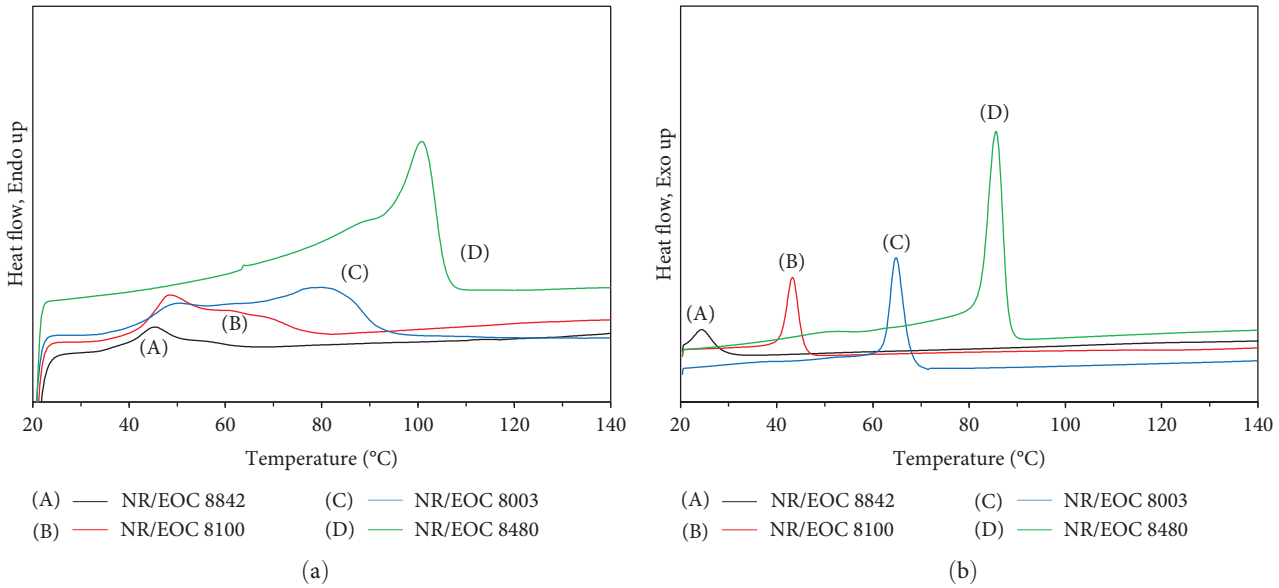

Figure 2: DSC thermograms of (a) second heating curve and (b) cooling curve of EOC phase in NR/EOC blends with various crystallinity of EOC.

Table 3: DSC parameters of EOC phase in NR/EOC blends with various ethylene content of EOC.

Parameters	NR/EOC (EOC grades)			
	8842	8100	8003	8480
Crystallization temperature (°C)	24.3	43.2	64.7	85.3
Melting temperature (°C)	45.8	65.7	80.5	101.0
Degree of crystallinity (%)	1.31	2.85	9.02	15.96

45–100°C according to the EOC used, as summarized in Table 3. The measured melting temperatures of crystalline fraction in the NR/EOC blends were used as a test temperature for the characterization of shape memory properties, which are related to the transition temperature of SMPs.

4.2. Effect of Ethylene Content of EOC on Mechanical Properties of NR/EOC Blends. The mechanical properties of the NR/EOC blends were measured by uniaxial extension performed at room temperature. Figure 3 displays the nominal stress–strain curves of NR/EOC blends with various crystallinity of EOC phase. It was found that a higher degree of crystallinity of EOC caused the NR/EOC blends with a larger slope of the linear portion of the initial stress–strain curve (approximately 0%–50% strain) or higher modulus of elasticity (Young's modulus) owing to the physical crosslinks formed by the crystalline phase of EOC in the NR/EOC blend. The modulus of elasticity can also be described as the resistance of material to being deformed elastically. Ideally, in the elastic regime, the material can fully recover its original shape after unloading. After the elastic regime, the irreversible process of plastic deformation occurs whenever stress exceeds a critical value and causes permanent changes in atomic positions. In the plastic deformation regime, the material cannot fully recover its original shape upon

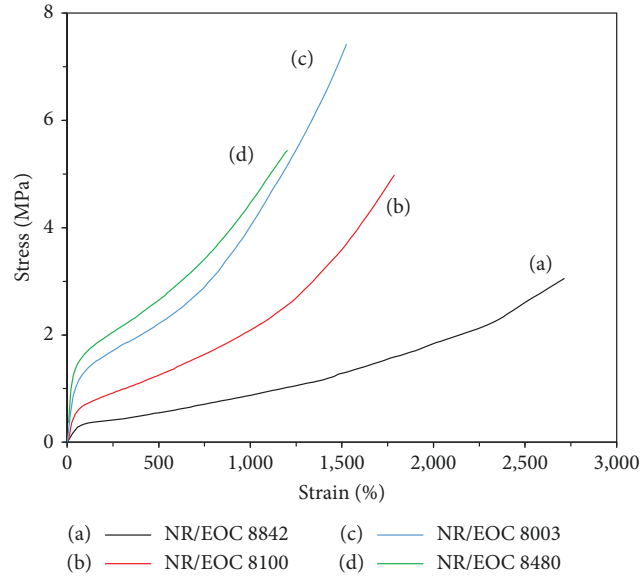

Figure 3: Stress–strain curves of NR/EOC blends with various ethylene content of EOC.

releasing an applied stress, and it can be observed by deviation from the straight-line portion of the initial stress–strain curve or yield point, which is the boundary between elastic deformation and plastic deformation.

The mechanical properties of the blends are summarized in Table 4. Modulus at 100% extension, tensile strength, and elongation at break of the NR/EOC blends were also summarized in Table 4. It was seen that the EOC crystalline phase provided stiffness and enhanced stress resistance to the NR/EOC blend. A higher degree of crystallinity of EOC in the NR/EOC blends showed the larger modulus and tensile strength of the NR/EOC blend with lower elongation at break, contributed by the stiff molecular chains.

Table 4: Mechanical properties of NR/EOC blends with various ethylene content of EOC.

Properties	NR/EOC (EOC grades)			
	8842	8100	8003	8480
Modulus of elasticity (kPa)	0.5 ± 0.1	10.3 ± 0.4	22.2 ± 0.3	38.8 ± 0.3
Elastic limit (%)	55 ± 2	50 ± 2	44 ± 1	33 ± 1
100% Modulus (MPa)	0.35 ± 0.00	0.68 ± 0.03	1.33 ± 0.03	1.67 ± 0.03
Tensile strength (MPa)	3.09 ± 0.07	5.07 ± 0.07	7.45 ± 0.08	5.48 ± 0.09
Elongation at break (%)	$2{,}730 \pm 45$	$1{,}808 \pm 13$	$1{,}524 \pm 12$	$1{,}212 \pm 15$

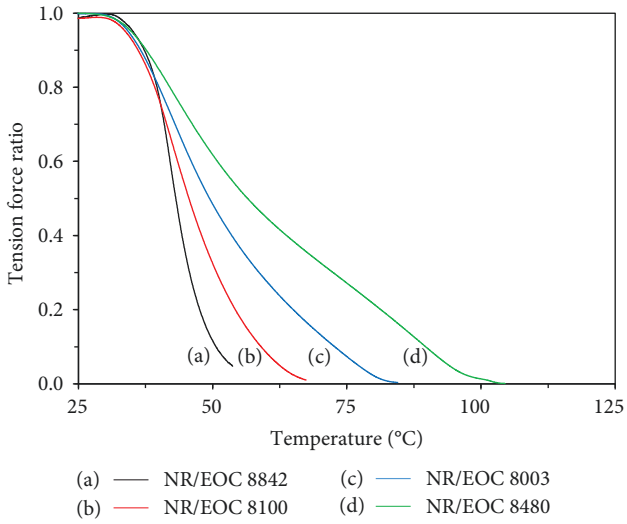

Figure 4: Nonisothermal relaxation of NR/EOC blends with various ethylene content of EOC.

4.3. TSSR Analysis. The thermo-mechanical behavior of the NR/EOC blends with various ethylene content of EOC phase was determined by the TSSR technique. The stress–temperature curve provides an idea regarding the thermo-mechanical behavior. The stress relaxation behavior takes place over a wider range of temperatures. It is mainly the presence of thermally reversible physical crosslinks. Figure 4 shows the results from TSSR in its non-isothermal condition. The relaxation curves strongly decrease with the scanned temperature, which is related to the relaxation of the molecular chain in the material. As seen in Figure 4, the decrease of force applied to the prepared NR/EOC blends at a constant magnitude of stain (50%) was different due to the comonomer content and crystallinity. The NR/EOC blend with lower ethylene content or crystalline fraction in the EOC phase exhibited higher relaxation than the NR/EOC blend with higher ethylene content. This is due to the crystalline fraction in the NR/EOC blend acting as a physical crosslinking and hindering the motion of the molecular chains. Also, they shifted toward higher temperatures with the ethylene comonomer content in EOC.

TSSR analysis provides the temperature transition points T_{10}, T_{50}, and T_{90} defined as a decrease of tensile force by 10%, 50%, and 90% from its initial value, respectively [20, 22]. The temperature transition points, as extracted from the curves of NR/EOC blends with various ethylene content of EOC, are summarized in Table 5. As a result, it can be clearly implied

Table 5: TSSR parameters of NR/EOC blends with various ethylene content of EOC.

Parameters	NR/EOC (EOC grades)			
	8842	8100	8003	8480
Initial stress (MPa)	0.08	0.30	0.82	1.28
Thermo elastic inversion (T_{10})	37.6	36.6	36.6	37.6
The set resistance (T_{50})	43.2	45.7	49.4	56.5
The material stability (T_{90})	50.7	59.1	72.8	89.7
TSSR index	0.75	0.66	0.59	0.56

that the ethylene comonomer content and crystallinity of EOC in the NR/EOC blends have a significant effect upon compression set resistance (T_{50}) and material stability (T_{90}), which is gradually increased with increase of the crystalline fraction in the blends. However, all the prepared NR/EOC blends exhibited the same behavior at the thermoelastic inversion point (T_{10}).

The TSSR index or RI that can signify the rubberlike behavior of a polymer is also included. The term "TSSR index" is calculated based on the area under the normalized force–temperature curve. A higher TSSR index value means a higher elasticity of the material. It can be indicated that the presence of octene copolymer along the ethylene copolymer backbone in EOC phase of NR/EOC blends provides the rubber-like properties to the blends [20].

4.4. Dynamic Mechanical Analysis. DMA results, Figure 5, showed only one peak in the loss factor (tan δ) curve as a function of temperature of the NR/EOC blends. The temperature at the tan δ peak is corresponding to the glass transition temperature (T_g) of the blends, which related to the molecular relaxation of the NR and EOC molecules. The loss factor peak showed that the decrease of ethylene content in the NR/EOC blends results a slightly shift of the T_g toward lower temperature. This is described by the lower thermal energy required to induce the mobility of the polymer chain (high chain flexibility) [23]. The T_g of the NR/EOC blends are also summarized in Table 6. Furthermore, it can be seen that the tan δ curve of blends dramatically increases at around 25–100°C. This is due to the motion of the polymer backbone owing to the transition from elastic region to the flow region of blends.

4.5. Morphology. The morphological observation of the prepared NR/EOC blends filled with $CaCO_3$ and TiO_2 was demonstrated by SEM technique. Figure 6 shows the BSE-SEM

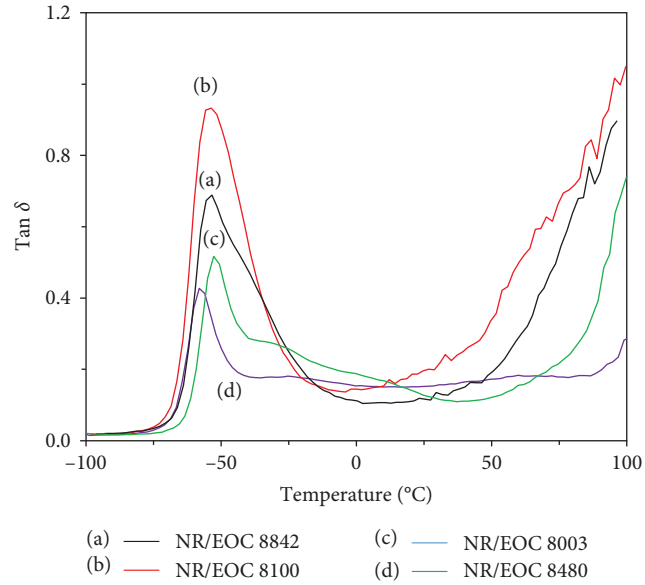

Figure 5: The damping factor (tan δ) as a function of temperature for the NR/EOC blends.

Table 6: The glass transition temperature at 5 Hz of NR/EOC blends with various ethylene content of EOC.

Parameters	NR/EOC (EOC grades)			
	8842	8100	8003	8480
Glass transition temperature	−58.17	−53.67	−53.42	−52.75

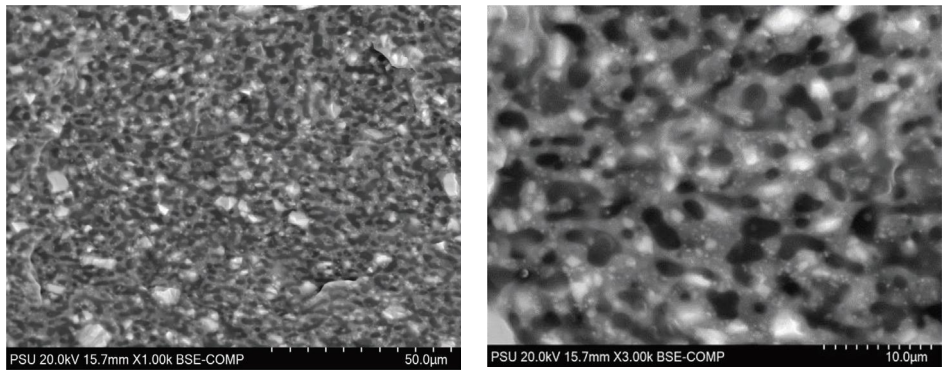

(a) (b)

Figure 6: SEM micrographs of NR/EOC blend at the magnitude of (a) 1,000x and (b) 3,000x.

micrographs of NR/EOC blend at the magnitude of (a) 1,000x and (b) 3,000x, respectively. It can be seen that the prepared NR/EOC blend showed a cocontinuous phase of NR and EOC. The NR phase strained with OsO_4 is shown in a lighter color, while the semicrystalline EOC phase is darker. Besides, the $CaCO_3$ and TiO_2 particles (approximately diameter of 2–10 μm in diameter) appear as bright spots in the SEM-BSE image due to high atomic number. It was found that the $CaCO_3$ and TiO_2 particles showed good dispersion and was mainly localized in the NR phase. Figure 7 shows the distribution of the $CaCO_3$ and TiO_2 particles in the NR/EOC blends with various ethylene content of EOC phase in NR/EOC blends. It was found that the $CaCO_3$ and TiO_2 particles showed good dispersion in all of NR/EOC blends.

4.6. SM Properties of EOC-Based NR/EOC Blends. The temperature at the end of melting of the thermoplastic segment from DSC analysis was used as the programing temperature or the testing temperature for further investigate the shape memory properties of NR/EOC blends with various ethylene content of EOC, as summarized in Table 7.

Figure 8 shows the SM properties in terms of shape fixity and shape recovery efficiencies of the NR/EOC blends with various ethylene content of EOC characterized at various

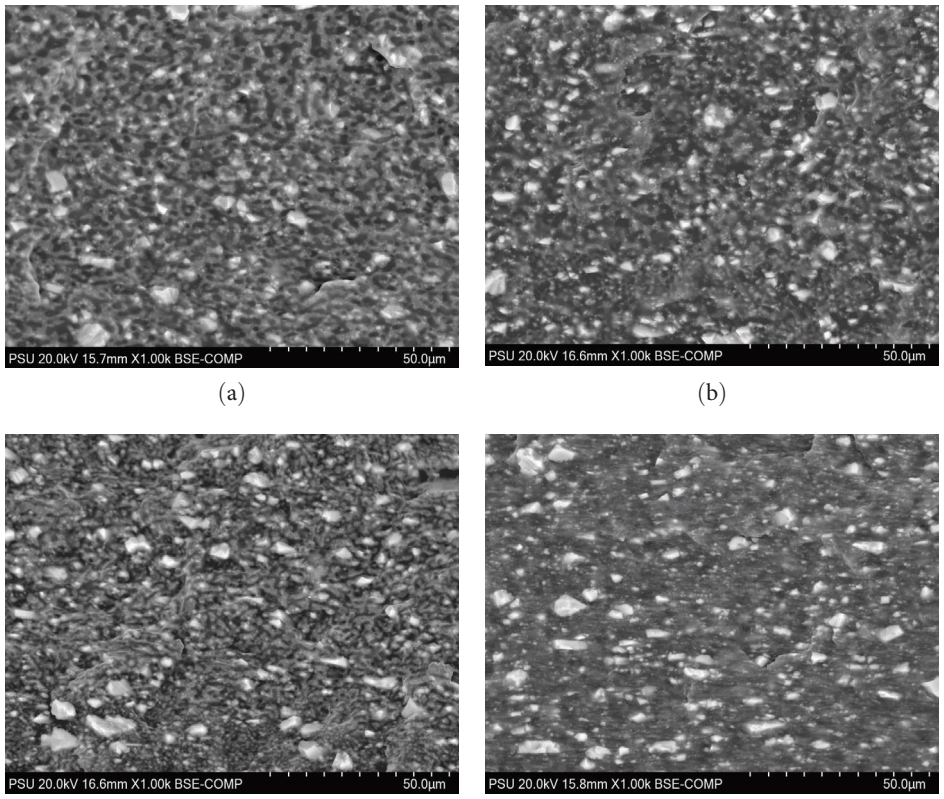

Figure 7: SEM micrographs (1,000x) of NR/EOC blends with grade (a) EOC 8842, (b) EOC 8100, (c) EOC 8003, and (d) EOC 8480.

Table 7: Programing temperature of NR/EOC blends with various ethylene content of EOC.

Parameters	NR/EOC (EOC grades)			
	8842	8100	8003	8480
Ethylene content of EOC phase in NR/EOC blends (wt%)	55	62	70	80
Programing temperature (°C)	60	89	94	107

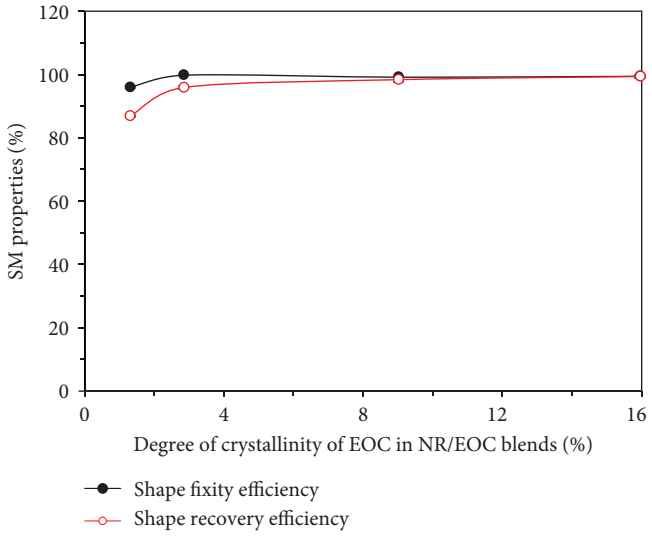

Figure 8: SM properties of NR/EOC blends at transition temperature with various ethylene content of EOC.

programing temperatures. The shape fixity and shape recovery efficiencies of the blends tended to increase with increasing of crystalline segments in the blends. In this present work, it was found that the SM properties of the prepared blends substantially exceed the best performance (close to 100%) by blending the NR/EOC at 50/50 parts by weight, having 62%–80% of ethylene content in the EOC phase which corresponding to approximately 3°–16° of crystallinity of EOC phase in the blends.

To proof the after repeated cycle of the prepared SMP, the cyclic test of SM properties of the NR/EOC blend was investigated for five cycles. The NR/EOC blend having 62 wt% of ethylene content in EOC phase was further investigated due to the satisfied SM performance with proper programing temperature (below the boiling point of water). The programing temperature used was 89°C. Table 8 shows the SM properties of the recyclable NR/EOC blend having 62 wt% of ethylene content in EOC phase. It was found that the shape fixity slightly decreased with the number of test cycles. The shape

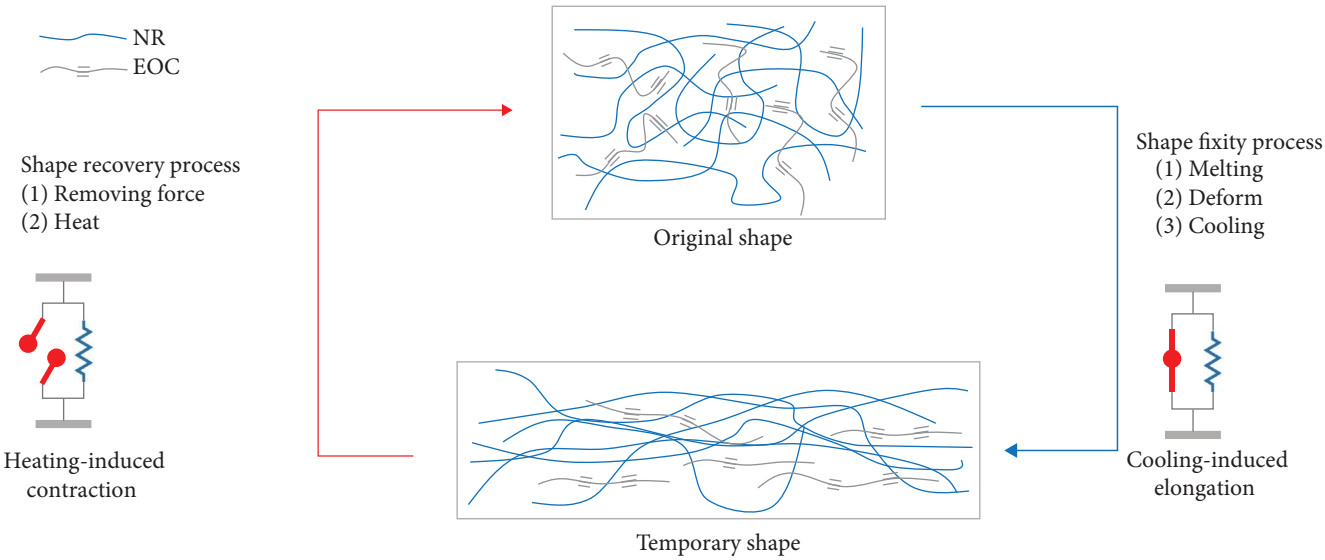

Figure 9: Proposed model of thermo-sensitive NR/EOC blend describing the shape fixity and shape recovery process.

Table 8: SM properties of recyclable NR/EOC blend having 62 wt% of ethylene content in EOC phase.

Cycle (N)	Shape fixity efficiency (%)	Shape recovery efficiency (%)
1	99.82 ± 0.10	95.95 ± 0.56
2	99.17 ± 1.46	89.45 ± 0.56
3	94.91 ± 0.15	77.34 ± 0.75
4	98.32 ± 0.35	69.78 ± 1.04
5	96.92 ± 0.21	70.31 ± 0.29

fixity efficiency of the blend decreased from 99.9% to 96.9% or approximately 3% after five times of the after repeated cycle. However, it was observed that the shape recovery efficiency of the blend significantly decreased after repeated cycles. The shape recovery efficiency decreased from 96.0% to 77.3% after three cycles of deformation and recovery process and was found to be constant at approximately 70% for four to five cycles of the after repeated cycles. This affirms well the superior SM properties of the prepared thermo-sensitive NR/EOC blends with different controllable transition temperatures, which are required to fill the demands of different environments (temperatures).

The proposed model to explain the mechanism of the prepared NR/EOC blends is depicted in Figure 9. The fixity and recovery of the material are controlled by the crystallized EOC segment, as well as chain entanglements in the amorphous NR phase. During the fixity process, the NR/EOC blend was subjected by an applied force to deform at the transition temperature of the reversible phase, and then the material was subsequently quenched. The EOC crystals occurred and oriented along the stretching direction during cooling [24, 25]. This ethylene segment in the EOC acts as a physically cross-linked network to immobilize or fix the deformed temporary network that is strong enough to resist the recovery force of the elastic network or chain entanglements until an appropriate stimulus (heat) is applied. In the recovery process, the elongated chain recovered due to the entropy elasticity of the amorphous NR phase when the heat was applied (heating-induced contraction).

5. Conclusion

The SMPs with superior SM properties were successfully fabricated with various controllable transition temperatures. Mechanical properties of NR/EOC blends showed an increasing trend as the crystallinity of EOC phase increased. The crystallization temperature, the melting temperature, and degree of crystallinity of the ethylene segment in the EOC increased as a function of ethylene content in the EOC. The TSSR analysis revealed that the relaxation curves shifted toward higher temperatures as the ethylene comonomer content in EOC increases. The set resistance and material stability of the NR/EOC blends were improved by the crystallized EOC phase. The shape fixity and shape recovery efficiencies of the blends tended to increase with increasing of crystalline segments in the blends. The shape fixity slightly decreased with the number of test cycles. However, the shape recovery efficiency scientifically decreased during reproducibility (30% efficiency reduction after five times of reproducibility). This study confirms that the temperature at the end of the melting peak of the crystalline phase in the SMP is a proper stimulus condition to promote the transition temperature of the SMP.

Data Availability

The data used to support the findings of this study are included in the article. Further data or information are available from the corresponding author upon request.

Conflicts of Interest

The authors declare that there are no conflicts of interest regarding the publication of this article.

Authors' Contributions

Ekwipoo Kalkornsurapranee was responsible for formal analysis, funding acquisition, supervision, validation, writing—review and editing; Adisak Keereerak was responsible for conceptualization, data curation, investigation, methodology, writing—original draft, writing—review and editing; Nussana Lehman and Akarapong Tuljittraporn were responsible for data curation, investigation, methodology, formal analysis, validation; Jobish Johns was responsible for formal analysis, supervision, validation, writing—review and editing, and Nattapon Uthaipan was responsible for conceptualization, formal analysis, project administration, methodology, resources, supervision, validation, writing—review and editing of the paper.

Acknowledgments

This research was supported by the Rubber Product and Innovation Development Research Unit (SCIRU63002), Faculty of Science, and Rubber Technology and Engineering Program, International College, Prince of Songkla University for facilities support. The authors also would like to thank the Faculty of Science Research Fund, Prince of Songkla University (Contract No. SCIEQUIP664001), for their equipment support in providing the internal mixer (CT-MX75-TQ).

References

[1] C. Liu, H. Qin, and P. T. Mather, "Review of progress in shape-memory polymers," *Journal of Materials Chemistry*, vol. 17, no. 16, pp. 1543–1558, 2007.

[2] G. Ehrmann and A. Ehrmann, "3D printing of shape memory polymers," *Journal of Applied Polymer Science*, vol. 138, no. 34, pp. 1–11, 2021.

[3] T. Chatterjee and K. Naskar, "Shape memory polymers based on EPDM/EOC blends," *RFP*, vol. 13, no. 3, pp. 1–11, 2018.

[4] T. Sengsuk, S. Intom, L. Songtipya, J. Johns, K. Chawengsaksopak, and E. Kalkornsurapranee, "Shape memory thermoplastic natural rubber for forensic applications," *IOP Conference Series: Materials Science and Engineering*, vol. 553, Article ID 012045, 2019.

[5] N. Lehman, L. Songtipya, J. Johns et al., "Shape memory thermoplastic natural rubber for novel splint applications," *Express Polymer Letters*, vol. 15, no. 1, pp. 28–38, 2021.

[6] A. Lendlein, H. Jiang, O. Jünger, and R. Langer, "Light-induced shape-memory polymers," *Nature*, vol. 434, no. 7035, pp. 879–882, 2005.

[7] T. Manouras and M. Vamvakaki, "Field responsive materials: photo-, electro-, magnetic-and ultrasound-sensitive polymers," *Polymer Chemistry*, vol. 8, no. 1, pp. 74–96, 2017.

[8] F. Pilate, A. Toncheva, P. Dubois, and J.-M. Raquez, "Shape-memory polymers for multiple applications in the materials world," *European Polymer Journal*, vol. 80, pp. 268–294, 2016.

[9] A. Lendlein and S. Kelch, "Shape-memory polymers," *Angewandte Chemie International Edition*, vol. 41, no. 12, pp. 2034–2057, 2002.

[10] X. Kuang, D. J. Roach, J. Wu et al., "Advances in 4D printing: materials and applications," *Advanced Functional Materials*, vol. 29, no. 2, Article ID 1805290, 2019.

[11] G. J. Berg, M. K. McBride, C. Wang, and C. N. Bowman, "New directions in the chemistry of shape memory polymers," *Polymer*, vol. 55, no. 23, pp. 5849–5872, 2014.

[12] A. M. Schmidt, "Electromagnetic activation of shape memory polymer networks containing magnetic nanoparticles," *Macromolecular Rapid Communications*, vol. 27, no. 14, pp. 1168–1172, 2006.

[13] W.-C. Chen, S.-M. Lai, M. Y. Chang, and Z.-C. Liao, "Preparation and properties of natural rubber (NR)/polycaprolactone (PCL) bio-based shape memory polymer blends," *Journal of Macromolecular Science, Part B*, vol. 53, no. 4, pp. 645–661, 2014.

[14] Y.-C. Chung, J. W. Choi, H. Y. Kim, and B. C. Chun, "The effect of pendant tertiary butyl group on the shape recovery of polyurethane copolymer under freezing," *Journal of Elastomers & Plastics*, vol. 45, no. 4, pp. 333–349, 2013.

[15] H. Liu, S.-C. Li, Y. Liu, and M. Iqbal, "Thermostimulative shape memory effect of linear low-density polyethylene/polypropylene (LLDPE/PP) blends compatibilized by cross-linked LLDPE/PP blend (LLDPE-PP)," *Journal of Applied Polymer Science*, vol. 122, no. 4, pp. 2512–2519, 2011.

[16] I. S. Kolesov and H.-J. Radusch, "Multiple shape-memory behavior and thermal-mechanical properties of peroxide cross-linked blends of linear and short-chain branched polyethylenes," *Express Polymer Letters*, vol. 2, no. 7, pp. 461–473, 2008.

[17] B. Heuwers, D. Quitmann, R. Hoeher et al., "Stress-induced stabilization of crystals in shape memory natural rubber," *Macromolecular Rapid Communications*, vol. 34, no. 2, pp. 180–184, 2013.

[18] F. Katzenberg and J. C. Tiller, "Shape memory effect, shock- and energy-absorption capability of critically cross-linked syndiotactic polypropylene," *Materials Today: Proceedings*, vol. 16, Part 3, pp. 1531–1537, 2019.

[19] ENGAGE™ Polyolefin Elastomers, "Available online:" (accessed on 12 october 2021) https://www.dow.com/content/dam/dcc/documents/en-us/catalog-selguide/777/777-088-01-engage-polyolefin-elasto mer-product-selection-guide.pdf?iframe=true.

[20] N. Uthaipan, B. Junhasavasdikul, N. Vennemann, C. Nakason, and A. Thitithammawong, "Investigation of surface properties and elastomeric behaviors of EPDM/EOC/PP thermoplastic vulcanizates with different octene contents," *Journal of Applied Polymer Science*, vol. 134, no. 21, pp. 1–10, 2017.

[21] E. Tekay, "Thermo-responsive shape memory behavior of poly (styrene-b-isoprene-b-styrene)/ethylene-1-octene copolymer thermoplastic elastomer blends," *Polymers for Advanced Technologies*, vol. 32, no. 1, pp. 428–438, 2021.

[22] F. F. Liu, Y. T. Sun, and Z. B. Wang, "Facile design of heat-triggered shape-memory ethylene-acrylic acid copolymer/chloroprene rubber thermoplastic vulcanizates," *Express Polymer Letters*, vol. 14, no. 3, pp. 281–293, 2020.

[23] A. Masa, H. Saito, T. Sakai, A. Kaesaman, and N. Lopattananon, "Morphological evolution and mechanical property enhancement of natural rubber/polypropylene blend through compatibilization by nanoclay," *Journal of Applied Polymer Science*, vol. 134, no. 10, pp. 1–14, Article ID 44574, 2017.

[24] J. Leng, H. Lu, Y. Liu, W. M. Huang, and S. Du, "Shape-memory polymers—a class of novel smart materials," *MRS Bulletin*, vol. 34, pp. 848–855, 2009.

[25] Y. Wu, J. Hu, J. Han et al., "Two-way shape memory polymer with "switch–spring" composition by interpenetrating polymer network," *Journal of Materials Chemistry A*, vol. 2, no. 44, pp. 18816–18822, 2014.